# Influence of Programming and Recovery Parameters on Compressive Behaviors of 4D Printed Bio-compatible PVC-PCL Blends

D. Rahmatabadi[a], M. Aberoumand[a], K. Soltanmohammadi[a], E. Soleyman[a], I. Ghasemi[b], M. Baniassadi[a], K. Abrinia[a], M. Bodaghi[c*] and M. Baghani[a*]

[a] *School of Mechanical Engineering, College of Engineering, University of Tehran, Tehran, Iran*

[b] *Faculty of Processing, Iran Polymer and Petrochemical Institute ,Tehran ,Iran*

[c] *Department of Engineering, School of Science and Technology, Nottingham Trent University, Nottingham, NG11 8NS, UK*

*Corresponding authors: mahdi.bodaghi@ntu.ac.uk; baghani@ut.ac.ir



## Abstract

This paper introduces a new class of bio-compatible shape memory polymers (SMPs) through blending PVC and PCL. The compressive shape-memory behaviors of 4D-printed SMP PVC with 5 and 10%wt of PCL are studied in detail. In this respect, a set of experiments are carried out to understand thermo-mechanical responses of PVC-PCL blends under various shape memory parameters like programming temperature, load holding time, applied strain and recovery temperature. DMTA and SEM imaging are also performed to provide thermal and morphological analyses. It is found that by raising the recovery temperature from 45 to 65°C, the shape recovery ratio increases from 5.63MPa to 7.92MPa when the PVC-PCL10 is programmed via the hot programming protocol. The highest level of shape fixity (100%) and the best performance of stress relaxation are achieved for hot programming sample, while the highest shape recovery ratio (100%) is obtained for cold programming. By applying the load holding time, the amount of shape fixity can reach from 88.14% to 100%. Results of this research are expected to provide an insightful understanding of the shape memory behaviors of PVC-PCL and be instrumental for 4D printing and programming of shape adaptive structures like shape-memory intervertebral cages as spinal support devices.

***Keywords:*** PVC-PCL blends; shape memory polymers; 4D printing; shape programming; bio-compatibility

This article has been accepted for publication and undergone full peer review but has not been through the copyediting, typesetting, pagination and proofreading process, which may lead to differences between this version and the Version of Record. Please cite this article as doi: 10.1002/adem.202400301.

## 1- Introduction

Additive manufacturing or 3D printing has attracted significant attention in various industries [1]–[4] for fabricating complex structures with a wide range of metallic, polymeric, and ceramic materials. In the field of medicine, however, 3D printing of polymers has made much more progress [5]–[7]. Shape Memory Polymers (SMPs) can restore an original shape (i.e., permanent shape) of an enormously deformed shape (i.e., temporary shape) when exposed to a suitable stimulus [8][9]. This intelligent feature is called Shape Memory Effect (SME) [10]. 3D printing of smart materials like SMPs is called 4D printing [11][12]. On top of 4D printing of SMPs, the working mechanism, stimuli and programming steps are the most prominent aspects of these polymers [13]. Joule heating is the most conventional stimuli which is also used in this research. The transition temperature of the polymers (glass transition temperature and melting temperature) is also an important player and acts as the switching temperature in the programming cycle [14]. The temperature and time dependent nature of polymers has led to program SMPs at the rubbery state or above melting temperature in most of the early investigations of SMPs which is called "hot programming (HP)" [15].

Nowadays, warm and cold programming are also used in glass and transition areas with the aim of reducing energy and time consumption [15][16]. Of course, provided that the polymer has the formability (beyond the elastic region) in these areas. The SME is defined by four terms: temporary shape, permanent shape, hard phase and soft phase in molecular architecture and morphology [16]. The hard phase can be chemical or physical crosslinks and molecular entanglements in amorphous polymers. On the other hand, glassy amorphous regions can be the soft phase in amorphous SMPs. In semi-crystalline polymers, crystals or chemical cross links can be hard phase and the soft phase is the glassy amorphous region or crystals in case of chemical cross-linked polymers [17].

In recent years, reports on SME in amorphous thermoplastics such as PC, PETG, PMMA and PVC have also been presented [16][18]. Considering the limitation of material in 4D printing, the use of these materials can be promising. Yang et al. [19][20] reported impression recovery of the indented fully amorphous PC and PMMA with a high dependency of their SME on programming temperature

as one of the findings. They also assumed that this smart behavior could be generalizable to all kinds of amorphous polymers. Wu et al. [21] found that the SME of the fully amorphous PC is highly dependent on programming temperature and imposed strain. Lower programming temperatures and higher imposed strains cause microcracks and damage in the PC SMP, while higher programming temperatures weaken SME. SME of PVC-based blends [22]–[25], and thermoset PVC networks [26][27] have been proved by some researchers.

Blending is one of the simple and practical ways to improve the properties of polymers [28][29]. Jeong et al. [25] obtained a good SME of the miscible blend of PVC/TPU with an acceptable molecular entanglement density between the PVC and polyester domain of TPU. They suggested that the hard phase of the TPU strengthens the net points resulting in a good SME. PVC shows a good affinity to polyesters like Poly(ε-caprolactone) (PCL). The miscible blend of PVC-PCL revealed an acceptable SME with the help of PCL crystallite as a reinforcement of the physical crosslinks [22][23]. The viscoelastic nature of the polymer's amorphous portion caused a stress relaxation phenomenon to be considered as a function of temperature and time. Stress relaxation, which deteriorates SME performance, could be limited by rigid backbones with restricted thermodynamical mobility and also increasing molecular weight. All the cited literature has introduced molecular entanglements, as net points to obtain SME for an amorphous and semi-crystalline polymer with a low degree of crystallinity. On the other hand, the use of PCL to soften PVC not only strengthens the shape memory property, but also makes its a candidate for more bio applications. The use of non-hygienic and low molecule additives in PVC, such as phthalates, especially diethylhexyl phthalate (DEHF), is a major challenge [30]. Because these materials do not establish a covalent bond with PVC and over time, they separate from PVC, especially in the fluid environment at a faster rate, and their degree of migration depends on the manufacturing parameters, the environment, and the amount of plasticizer.

Despite many applications of PVC in various industries and the evolution of 3D printing methods in the last two decades, one of the manufacturing challenges is 3D/4D printing of PVC parts. Of course, limited research has been done on the printing ability of PVC and improving the printing

conditions in terms of rheology. The use of a bio-compatible polymer such as PCL, in addition to improving the properties of shape memory and softening PVC, can also have a positive effect on the development of its 3D/4D printing. One of the main advantages of 4D printing is the automatic assembly capability, which reduces cost and time. The combination of 4D printing and cold and warm programming bio-compatible PVC-PCL highlights this advantage especially in medical applications, provided that the SMP has a high formability.

This paper, for the first time, introduces a successful 4D printing method of PVC-PCL blends and comprehensively investigates their wide usability and shape memory properties. Effects of programming parameters such as programming temperature, load holding time, applied strain and recovery temperature were examined. Shape recovery was conducted in free and constrained manners so that all SME parameters, including shape fixity, shape recovery, stress recovery and stress relaxation, were quantitatively examined and presented. In addition, DMTA and SEM imaging were applied for thermal and morphological analyses. Their implications on the shape memory effect of 4D printed PVC-PCL blends are then put into evidence, and pertinent conclusions are outlined. Due to the absence of similar results in the specialized literature, this paper is likely to fill a gap in the state-of-the-art 4D printing of PVC and contribute to a better understanding of the behavior of 4D printed PVC-PCL blends towards an efficient design of shape adaptive composite structures like shape-memory intervertebral cages as spinal support devices.

## 2- Materials and Methodology

### *2-1- Parent materials*

Commercial non-toxic food grade PVC granules prepared by Pishro Plast Bespar Co. with a K value of 65 and PCL prepared by eSun Co. (China) were selected as the parent materials. This PVC grade have inherent viscosity of 0.88 dL/g, $M_n$= $38.5\times10^3$ g/mol, $M_w$=$78.0\times10^3$, and PDI about 2 [31].

### *2-2- Processing*

For this research, the PVC-PCL samples were made and fabricated in the three main stages of blending, producing filament, and 3D printing. The preparation of PVC-PCL blend samples was done using two combinations of 5%wt and 10%wt of PCL (denoted by PVC-PCL5 and PVC-PCL10) with an internal mixer. At first, PVC granules were poured into the internal mixer at a temperature of 183 °C for 8 minutes, and then PCL was added, and the PVC-PCL blend was mixed for 8 minutes at 100 rpm. The PVC-PCL granules were obtained by crushing hot-pressed thin sheets which were made of PVC-PCL lumps from blending to prepare the filament with an extruder. In Figure 1, a schematic of the filament production processes and FDM printed structures is presented.

### *2-3- 3D printing*

Lab-made extruder with an L/D ratio of 15 and 3D printer with fused filament fabrication (FFF) technology were used to prepare PVC-PCL filaments and samples, respectively. The specifications of the preparing filament process and printing of the samples are presented in Table 1.

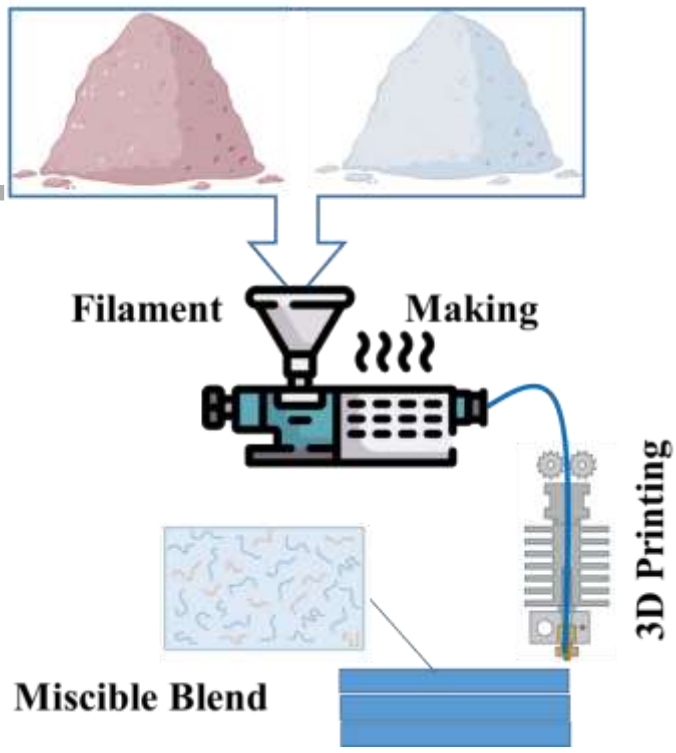


**Figure 1.** Schematic of the filament production process and 3D printing

**Table 1.** Filament preparation and 3D printing parameters for PVC-PCL blends.

| | |
|---|---|
| Extrude temperature (°C) | 200 |
| Extrude speed (RPM) | 25 |
| Nozzle temperature (°C) | 200 |
| Bed temperature (°C) | 60 |
| Velocity (mm/s) | 10 |
| Raster | 0 |
| Number of walls | 1 |
| Layer thickness (mm) | 0.2 |
| Nozzle Diameter (mm) | 0.8 |

### *2-4- Thermal analysis*

To specify the different thermal zones and evaluate the thermomechanical behavior of PVC-PCL blends Dynamic mechanical thermal analysis (DMTA) was performed (ASTM D4065-01 standard) by a dynamic mechanical thermal analyser (Mettler Toledo, Switzerland). Geometry, frequency, thermal range, heating rate and loading mode were selected as 40mm×10mm×1mm, 1 Hz, -100°C-100°C, 5°C/min and three-point bending, respectively.

### *2-5- SEM*

SEM imaging was used to study the morphology and miscibility of PVC-PCL blends. To ensure brittle fracture, the samples were broken in liquid nitrogen and the cross-section fracture was covered with gold, and then SEM imaging was done.

### *2-6- 4D printing*

The shape memory properties of PVC-PCL blends including shape fixity, shape recovery, stress recovery and stress relaxation were assessed by considering the parameters of shape memory cycle such as programming temperature, load holding time deformation and recovery temperature under compression loading. To investigate these parameters, two different constrained and unconstrained recovery processes were performed. In Figure 2, the schematics of the programming process at different temperatures (cold, warm and hot) and recovery with free and constrained protocols for PVC-PCL10 compound are presented. All shape memory test samples were printed in the same dimensions of 10×10×10 mm. All the important parameters to go through the shape memory cycle are presented in Table 2.

**Table 2.** Shape memory cycle conditions for PVC-PCL blends in the compression loading mode.

| Materials | PVC-PCL5 | PVC-PCL10 |
|---|---|---|
| Holding time for relaxation (s) | 240 | 240 |
| Loading temperature (°C) | 80 (Hot) | 25, 45, and 65 (cold, warm, and hot) |
| Deformation (%) | 40 | 40 and 80 |
| Load holding time (s) | 0 | 0 and 600 |
| Holding time for freezing (s) | 120 | 120 |
| Loading rate (mm/min) | 3 | 3 |
| Heating rate (°C/min) | 15 | 15 |
| Cooling rate (°C/min) | 30 | 30 |
| Recovery temperature (°C) | 80 | 45 and 65 |

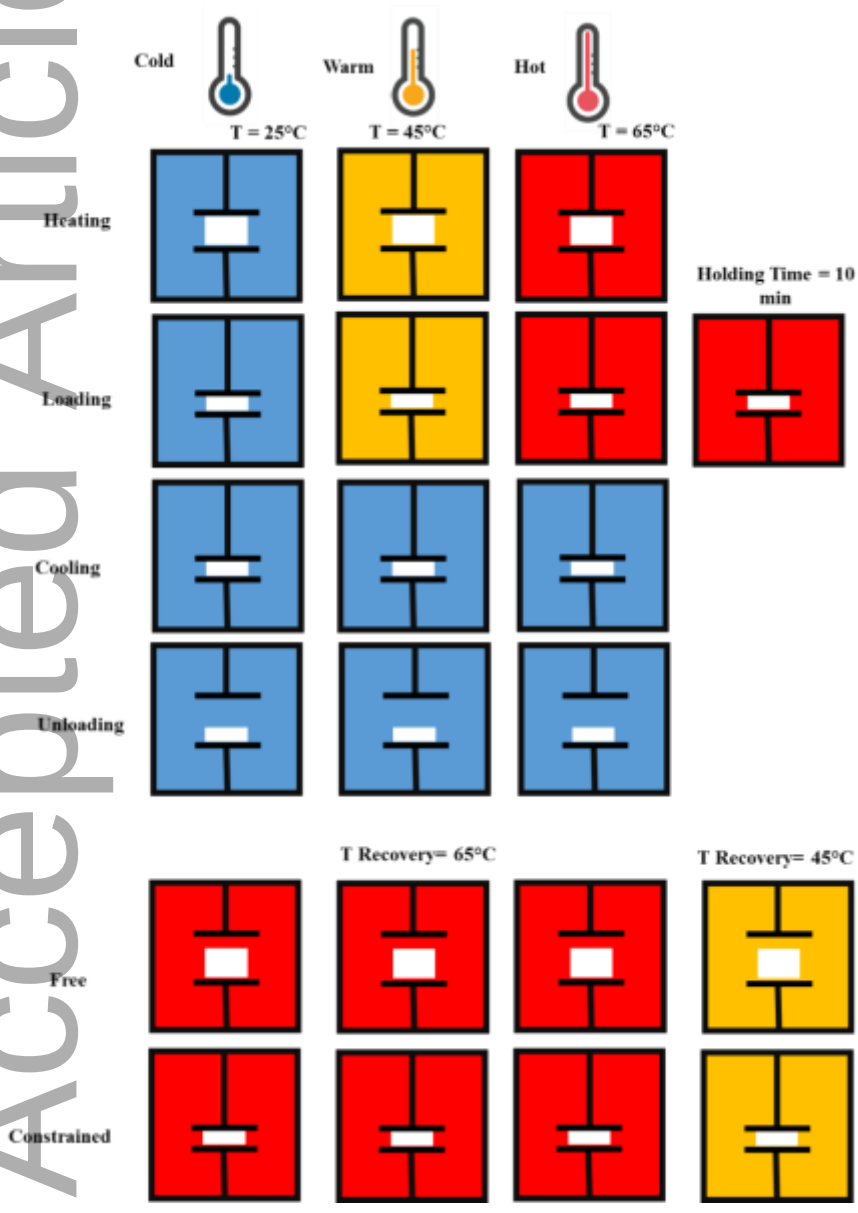


**Figure 2.** Schematic of the programming process at different temperatures and recovery with free and constrained protocols

## 3- Results and discussion

### *3-1- DMTA*

Figures 3 and 4 show changes of storage modulus and Tanδ as the DMTA results for unprocessed polymers (PVC and PCL) as well as PVC-PCL blends with two different compositions (PVC-PCL5 and PVC-PCL10), respectively. According to Figure 3, glass-to-rubber transition zone for PVC starts at 55°C and continues to 78°C. Also, the middle of the storage modulus is detected at 65°C, which represents the glass transition temperature. In this thermal range, the storage modulus decreases from 511MPa to 16.5MPa. Also, Figure 3 demonstrates the changes of storage modulus in the -100°C to 100°C for PCL. PCL has a glass-to-rubber transition zone in the temperature range of -65 to -30°C, in which the drop of the elastic modulus is more obvious than the peak of the Tanδ. In the following, the extreme peak of storage modulus drop occurs in a narrow thermal range, and temperature of 60°C is considered as the melting temperature. In this period, the storage modulus drops sharply and tends to zero with a high slope.

According to Figures 3, both PVC-PCL samples have a sharp modulus drop with a continuous decreasing trend and a severe decreasing rate. Figure 4 also confirms that only one Tanδ peak is observed throughout the thermal range that includes the melting point and transition of PCL and transition of PVC [22]. These results indicate the high compatibility and solubility of raw PVC and PCL polymers and the obtaining of miscible PVC-PCL blends. The high intermolecular interaction and compatibility and the closeness of the solubility parameters of polyesters such as PCL and PCL-based TPU and chlorinated polymers such as PVC cause the high rate of miscibility of their blends, which has already been discussed [22][24][32][33]. With the addition of 5%wt. and 10%wt. PCL, the starting temperature of the sharp drop of storage modulus decreases by 10°C and 35°C. Also, the glass-to-rubber transition zone becomes wider for PVC-PCL compounds, and with the increase of PCL amount, more intensity is observed. According to Figure 4, Tanδ peak for PVC and softened PVC with 5%wt. and 10%wt. PCL are identified at 72°C, 63°C, and 52°C, respectively. Also, in

order to investigate the properties of shape memory effect in different thermal regions, the DMTA results are quantitatively summarized in Table 3.

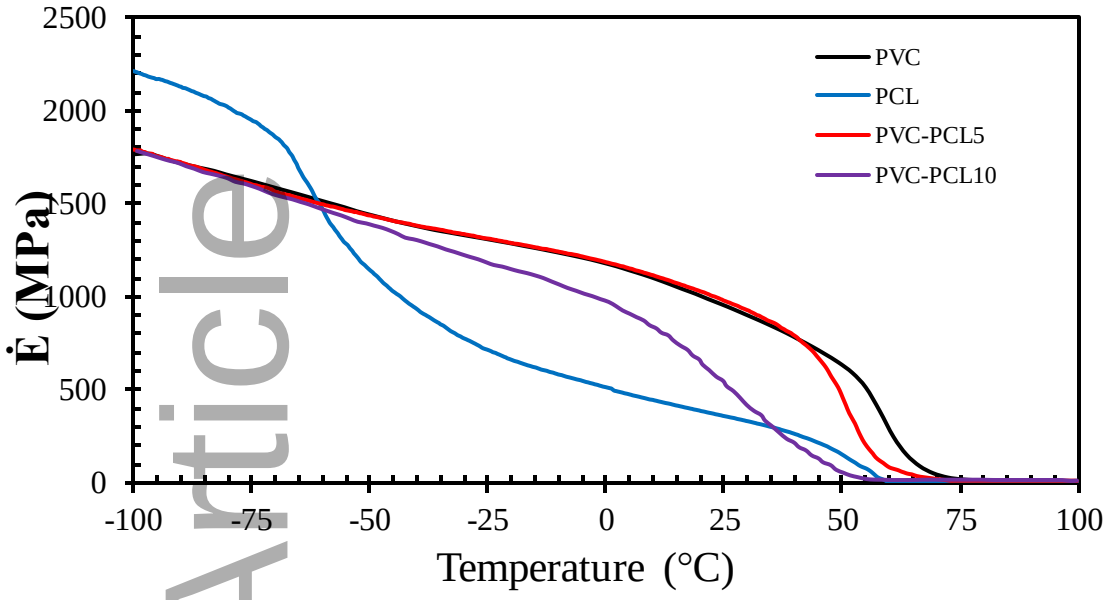


**Figure 3.** Storage modulus of the 3D printed PVC-based composite samples.

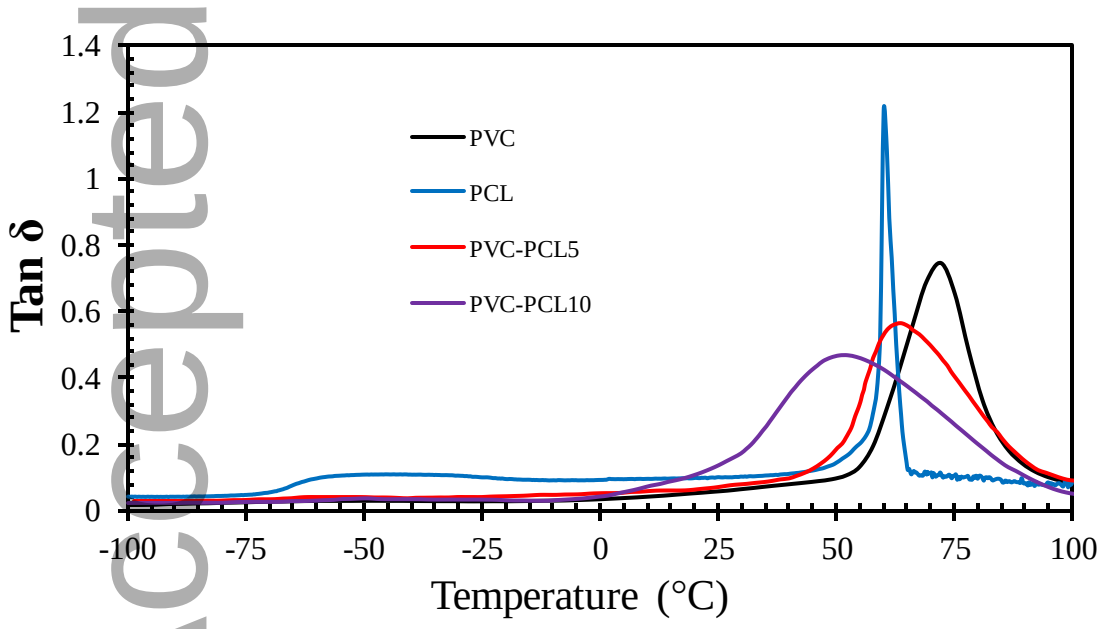


**Figure 4.** Tanδ of the 3D printed PVC-based composite samples.

**Table 3.** Summary of the DMTA results for PVC and PVC-PCL composite blends.

| Materials | Storage Modulus | | | Tanδ | |
|---|---|---|---|---|---|
| | Storage Modulus Range (MPa) | Temperature Range (°C) | Middle Temperature (°C) | Peak Value | Temperature (°C) |
| **PVC** | 510.9-12.3 | 55-78 | 65 | 0.74 | 72 |

| | | | | | |
|---|---|---|---|---|---|
| **PVC-PCL5** | 1667.1-14.6 | 40-65 | 50 | 0.56 | 63.5 |
| **PVC-PCL10** | 807.4-22.3 | 15-55 | 33 | 0.47 | 52.6 |

### *3-2- Shape memory cycle*

Figure 5 shows the shape memory cycle steps, which include three steps (1) heating and loading, (2) cooling and unloading, and (3) recovery. According to Figure 5, the recovery stage has been performed with two protocols and different recovery temperatures (45 and 65°C for PVC-PCL10). This work is to examine the stress recovery performance of the samples at two different working temperatures. As can be seen, with an increase in temperature, the amount of stress recovery is increased. But what makes the recovery step superior at a lower temperature is the better stress relaxation behavior compared to high temperatures. Also, according to the bio-compatibility of PVC and PCL as raw materials of the PVC-PCL blend, its performance in the temperature range close to body temperature is important. In Figure 6, the load holding time as a subset of the loading step that is done after loading and before cooling is presented. This parameter also plays an essential role in the shape memory cycle and strongly affects SME. All these steps are discussed in more detail below.

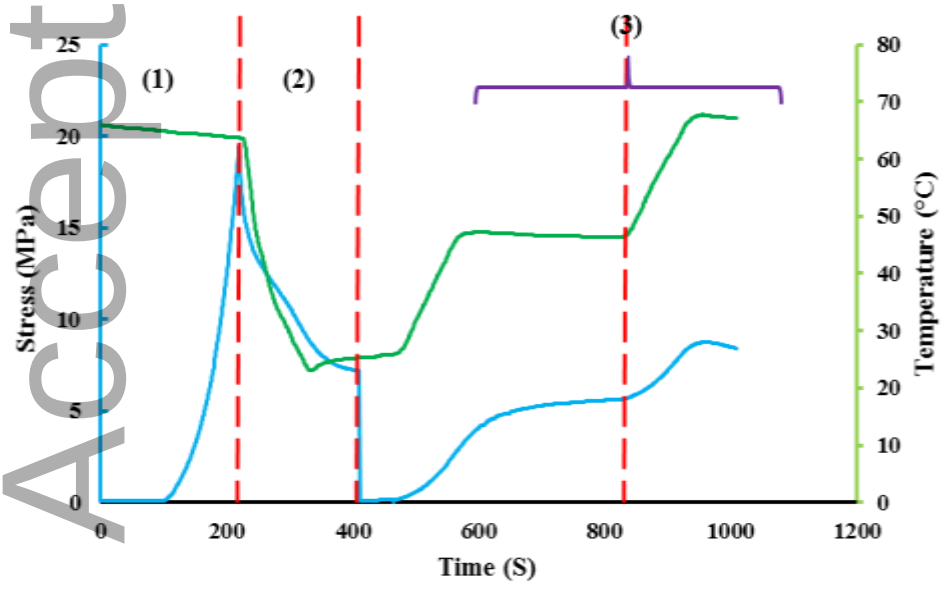


**Figure 5.** Shape memory cycle steps: (1) heating & loading, (2) cooling & unloading, and (3) recovery process with the protocol of increasing the temperature to 45°C, maintaining at 45°C and increasing again to 65°C.

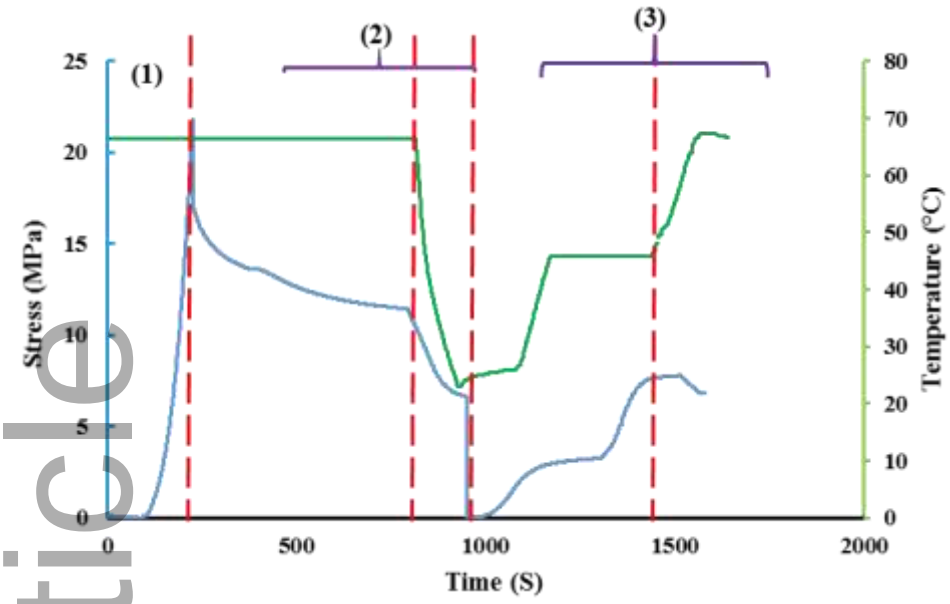


**Figure 6.** Shape memory cycle steps: (1) loading, (2) load holding time, cooling, and unloading, and (3) recovery process with the protocol of increasing the temperature to 45°C, maintaining at 45°C and increasing again to 65°C.

### *3-3- Programming*

The effect of programming temperature on shape memory performance for miscible PVC-PCL blends using constrained and free tests under compression loading mode was investigated. This investigation includes programming and recovery steps of the shape memory cycle. In Figure 7, the compressive stress-strain diagrams are presented in three glassy, transition, and rubbery heat zones for PVC-PCL5 and PVC-PCL10. Based on the results, both compounds have similar behavior in three thermal regions. Glassy polymers show linear elastic behavior, yielding, strain softening, and strain hardening strain when strain is applied, which can be observed in both compressed compounds at ambient temperature in the order of these stages. Of course, the intensity of each area depends on parameters such as free volume, distribution, and even printing parameters. The values of yield stress in the glassy region for PVC-PCL5 and PVC-PCL10 compounds are read 52.07MPa and 39.71 MPa, respectively. The compressive stress-strain behavior in both the transition and rubbery regions is completely elastic, with a difference that increasing the temperature causes a decrease in the elastic

modulus and the slope of the linear region. For this reason, the slope of the elastic region and yield stress in the warm programmed sample is more than hot.

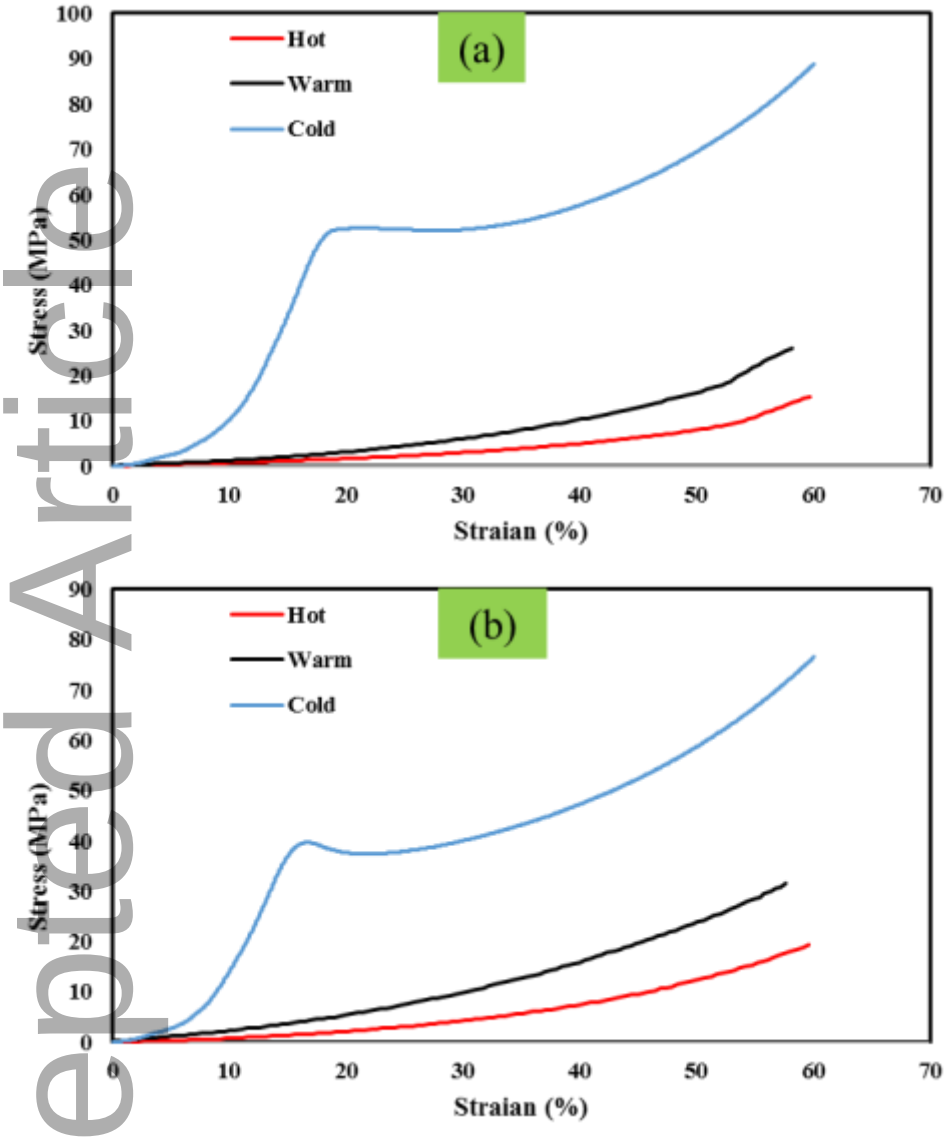


**Figure 7.** Compression programming in terms of stress-strain at cold, warm, and hot programming for (a) PVC-PCL5 and (b) PVC-PCL10.

### *3-4- Shape fixity and recovery*

#### *3-2-1- Effect of programming temperature and composition*

To investigate the effect of programming temperature on SME, PVC-PCL5 and PVC-PCL10 compounds were programmed at three temperatures ($T_g$-20°C,~ $T_g$ , $T_g$+20°C) as cold, warm, and hot programming.

In Table 4, the values of shape fixity and shape recovery for both PVC-PCL compounds in three programmed thermal zones are presented. As can be seen, the shape memory performance of two compounds in different thermal regions has the same trend, so that in the rubber region, the highest values of shape fixity are obtained, and on the opposite side, the samples programmed at ambient temperature have the highest shape recovery ratio. The samples programmed in the transition region also show intermediate shape memory performance. Also, in all three thermal regions, the shape fixity values are higher for the PVC-PCL5 compound, and on the other hand, except for the samples programmed at ambient temperature, where both PVC-PCL compounds have full shape recovery (100%), the shape recovery ratios are higher for the PVC-PCL10 compound. Of course, the effect of programming temperature on shape memory properties is much more visible and tangible than the effect of chemical composition in PVC-PCL blends.

The programming in different thermal zones strongly affects the deformation, shape fixity, and shape recovery mechanisms. In the glassy thermal region, due to the limitation in free volume and molecular mobility, as well as the heterogeneous distribution of free volume, all polymer chains do not participate in deformation and shape memory cycle processes, and polymer chains are divided into three parts with completely different behavior: elastic, viscoelastic, and plastic. In addition to the elastic part, which is released immediately after unloading, the viscoelastic area is also released over time, and this factor causes the reduction of shape fixity ratio in the samples programmed at ambient temperature [15][16][34]. The values of shape fixity for cold programmed PVC-PCL5 and PVC-PCL10 compounds are read 61.69% and 54.04%, respectively. In other words, the free volume distribution in the glassy state causes the anisotropic shape change and the limited local participation of the polymer chains in the shape memory cycle. Also, the application of high deformation to the polymer in the glassy range is accompanied by the limitations of molecular mobility and free volume, which causes changes in the length and angle of atomic bonds [15][35]–[37]. This phenomenon causes greater instability and increases the internal energy of the polymer system [38]. By increasing the temperature in the recovery stage, the energy required to return to the original form (thermodynamic equilibrium

of the polymer system) is provided and due to the higher instability in the deformed state, the recovery of the original shape is done faster and at lower temperatures. For this reason, complete recovery is obtained at a high rate for both PVC-PCL compounds in cold programming.

Hot programming is done in the rubbery heat zone and has the main differences from cold programming. Among the most important parameters, we can point out the uniform distribution of free volume, high molecular mobility, the participation and elongation of most polymer chains, the creation of an isotropic spatial shape, and a strong decrease in entropy. In fact, in the rubbery region, the necessary energy for molecular movement, loosening of physical net points, and stretching of chains is provided so that their spiral and random form takes a new elongated structure. Also, more stability (thermodynamic equilibrium) in this case due to the transition from the rubber to the glass region and the entrapment of the elastic entropy leads to the achievement of high shape fixity. The amount of shape fixity for hot programmed PVC-PCL5 and PVC-PCL10 are 97.37% and 88.14%, respectively. In addition, the hot programmed samples show an acceptable shape recovery in the rubbery heat zone.

The programmed samples in the transition thermal zone between glassy and rubbery, which is called the transition zone, have an intermediate behavior with a greater tendency to hot programmed samples. In fact, warm programmed samples show a more balanced behavior in that they have neither weak shape fixity like cold programmed samples nor moderate shape recovery like hot programmed samples. Shape recovery values for PVC-PCL5 and PVC-PCL10 compounds programmed in the transition thermal zone are calculated 89.70% and 98.34%, respectively.

**Table 4**. SEM results for the effect of programming temperature in the bending mode.

| Materials | Cold | | Warm | | Hot | |
|---|---|---|---|---|---|---|
| | Shape Fixity (%) | Shape Recovery (%) | Shape Fixity (%) | Shape Recovery (%) | Shape Fixity (%) | Shape Recovery (%) |
| **PVC-PCL5** | 61.69 | 100 | 71.56 | 89.70 | 97.37 | 86.26 |
| **PVC-PCL10** | 54.04 | 100 | 66.55 | 95.34 | 88.14 | 91.05 |

### *3-2-2- Effect of load holding time, deformation, and recovery temperature*

In Table 5, the values of shape fixity and shape recovery are presented for PVC-PCL10 by programming in three different thermal zones and considering the effect of load holding time and the amount of deformation in two recovery temperatures. As mentioned in the previous section, with the increase in programming temperature, the shape fixity ratio increases greatly. The shape fixity values for cold, warm, and hot programmed samples are 54.04%, 66.55%, and 88.14%, respectively. Increasing the programming temperature increases the free volume, its more uniform distribution, and the participation of more polymeric chains, and increases the thermodynamic stability, which requires a higher recovery temperature or a long recovery time for more and better shape recovery. For this reason, by increasing the recovery temperature from 45°C to 65°C, the shape recovery ratio increases, and this increment is more severe for the hot programmed sample.

According to the results of Table 5, taking into account 10 minutes' load holding time, the amount of shape fixity reaches 100%, and on the other hand, the amount of shape recovery decreases. Applying the load holding time creates conditions for the stability and balance of the deformed shape after the deformation, which increases the thermodynamic stable state. Applying load holding time activates two mechanisms of structure relaxation and stress relaxation. The first mechanism causes an increase in the thermodynamic stable state, which increases shape fixity and decreases shape recovery. By applying the load holding time, the amount of shape fixity reaches from 88.14% to 100% and the shape recovery also decreases in both recovery temperatures. The amount of shape recovery at 45°C to 65°C decreases by 36.93% and 22.16%, respectively. In addition, by considering the load holding time, the opening possibility of physical entanglements in the rubbery zone increases, and in this way, it is effective in reducing shape recovery.

Another effective parameter in the programming process is the degree of deformation. According to Table 5, with the increase of deformation from 40% to 60%, the shape fixity decreases from

91.03% to 88.14%. This decreasing trend in shape recovery is also observed in both recovery temperatures. The increase of strain higher than 40% in programming occurs in the strain-hardening region, which is associated with more stretching of polymer chains. This phenomenon at higher temperatures especially at rubbery can cause chain slippage and also open physical net points. These interactions justify the decrease in shape memory performance with the increase in applied deformation.

**Table 5.** PVC-PCL10 SEM results for the effect of programming temperature, load holding time, and amount of deformation at two recovery temperatures.

| Conditions | Shape Fixity (%) | Shape Recovery at 45C° | Shape Recovery at 65C° |
|---|---|---|---|
| Hot | 88.14 | 65.77 | 91.05 |
| Warm | 66.55 | 86.69 | 95.34 |
| Cold | 54.04 | 92.25 | 100 |
| Hot with holding time | 100 | 41.48 | 70.87 |
| 40% hot Programmed | 91.03 | 66.64 | 95.08 |

### *3-5- Stress recovery and relaxation*

#### *3-5-1- Effect of programming temperature and composition*

In Figure 8, stress recovery changes according to temperature and time for the PVC-PCL5 blend are demonstrated for two hot and warm programmed samples. According to Figure 8(a), for a more detailed analysis, the stress recovery diagrams of PVC-PCL5 can be divided into three regions (from the ambient temperature to the transition temperature; from the transition temperature to the end of the recovery temperature and after recovery).

In the first region (recovery temperature up to 55°C) the warm and hot programmed PVC-PCL5 samples have the same behavior. In the second region, the recovery behavior of the two samples is completely different, so the slope of the stress recovery with increasing temperature is much more intense for the warm programmed sample. Also, the maximum value of the stress recovery for the

warm programmed sample is higher and obtained at a lower temperature compared to the hot programmed sample. According to Figure 8(b), in the third region, which is the investigation of the stress recovery behavior after the maximum value, the hot programmed sample shows a better stress relaxation performance and the stress relaxation rate at the maximum recovery temperature (constant temperature of 80°C) during the time is lower than the warm programmed sample.

Quantitative results of these Figures are extracted and presented in Table 5. According to the results, the maximum stress recovery for PVC-PCL5 in the warm programmed sample is 10.43 MPa, obtained at 70°C, while this value is 8.19 MPa for the sample hot programmed at 80°C. As it has been discussed earlier, programming at lower temperatures, particularly lower than the average $T_g$ causes inhomogeneous strain propagation in limited sites that possess favourable freedom to conformational changes [39]–[41]. Besides, these conformational changes result in a burst in free volume proportion and size [42]. Hindered molecular mobility at lower temperatures causes a considerable elastic strain to be stored in limited chains with an immense order of non-equilibration in the deformed conformation. Therefore, these regions with a high concentration of more mobile nonequilibrium chains tend to relive their stored internal energy in greater values at higher speeds as well as lower peak temperatures. It is due to the higher stored internal energy by a non-equilibrated polymer system to altered macromolecule bond length and angle [41][43]. For this purpose, the maximum value of the recovery stress for the warm programmed sample is obtained at a lower temperature, and the increase in temperature causes an increase in the stress relaxation rate.

Figure 9 illustrates the stress recovery diagram for PVC-PCL10 in terms of temperature and time. Considering the recovery temperature of 45°C for this compound, which is its glass transition zone, the stress relaxation rate is very low, and it can be the excellent performance for medical applications in the body temperature range. Therefore, by reducing the recovery temperature, the stress relaxation can be overcome.

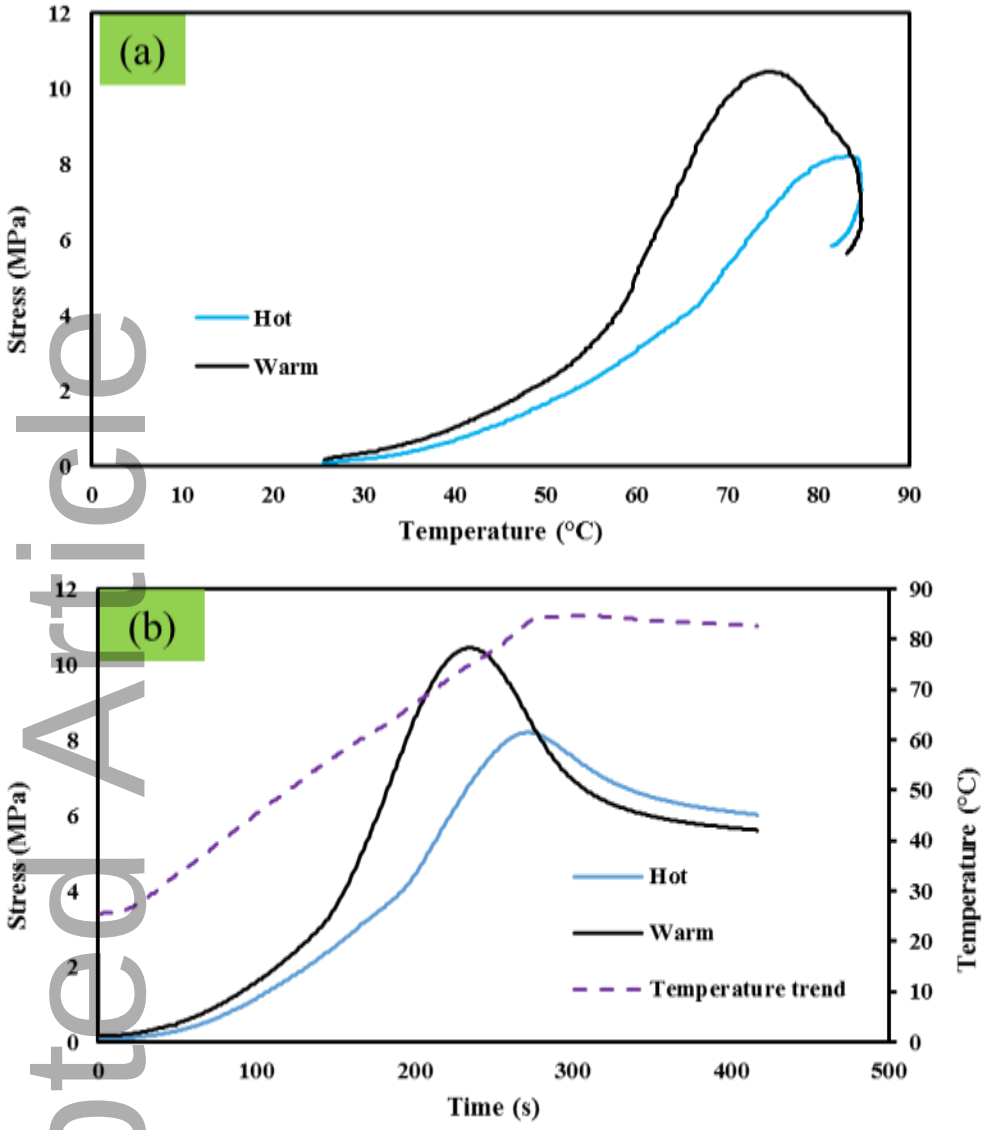


**Figure 8.** Stress recovery for hot and warm programmed PVC-PCL10 samples in terms of (a) temperature and (b) time.

**Table 6.** Maximum stress recovery values for PVC-PCL5 samples programed at different temperatures.

| Conditions | Max Stress Recovery at 80°C (MPa) | Stress Recovery at end of 80°C (MPa) |
|---|---|---|
| Hot | 8.19 | 5.81 |
| Warm | 10.43 | 5.95 |
| Cold | 9.88 | 5.87 |

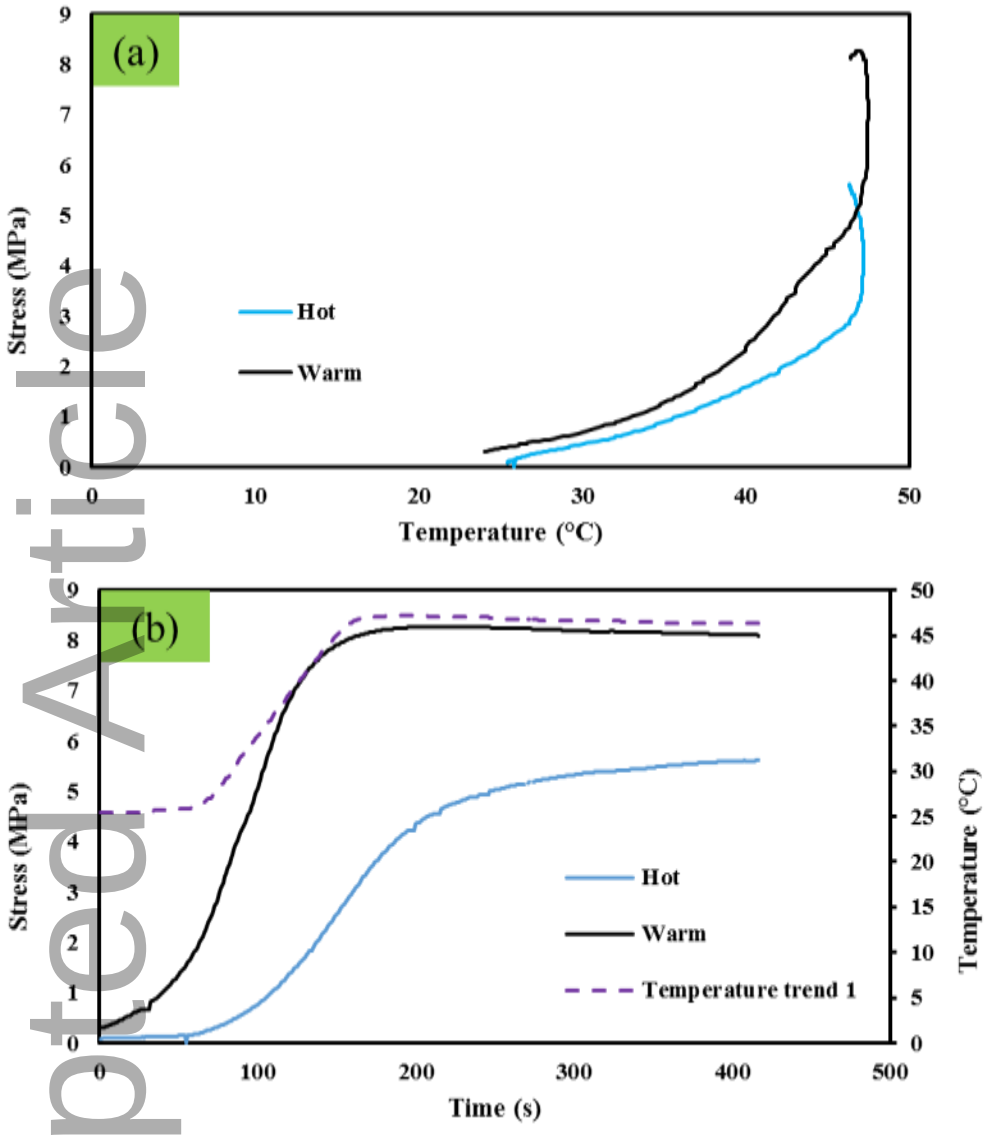


**Figure 9.** Stress recovery for hot and warm programmed PVC-PCL10 samples in terms of (a) temperature and (b) time.

**Table 7.** Maximum stress recovery values for PVC-PCL10 samples programmed in different conditions and temperatures.

| Conditions | Max Stress Recovery at 45°C (MPa) | Stress Recovery at the end of 45°C (MPa) | Max Stress Recovery at 65°C (MPa) | Stress Recovery at the end of 65°C (MPa) |
|---|---|---|---|---|
| Hot | 5.63 | 5.63 | 8.74 | 8.43 |
| Warm | 8.28 | 8.15 | 5.34 | 3.89 |
| Cold | 8.01 | 7.84 | 6.12 | 5.87 |
| Hot with holding time | 3.26 | 3.26 | 7.72 | 6.01 |
| 40% hot Programmed | 3.28 | 3.28 | 5.28 | 4.9 |
| Recovery at 65 | *** | *** | 7.92 | 7.15 |

### *3-5-2- Effect of programming deformation*

The value of applied deformation in the programming stage is another basic and influential parameter for the stress recovery. Figure 10 displays the stress recovery changes in terms of temperature and time for two samples programmed with 40% and 60% deformations under compression loading. Based on Figure 10(a), with the start of the recovery process (heating), the amount of stress recovery is released for the sample with less applied strain (40%) even at low temperatures, while for the 60% applied deformation sample, the recovery process starts at 45°C. In other words, the amount of stress recovery up to 45°C is higher for the programmed sample with lower strain. This phenomenon is caused by more thermodynamic equilibrium because the loading time is longer in the sample with 60% applied strain in the rubbery region. At the first recovery temperature (45°C), the amount of stress recovery increases continuously over time at a low rate and stress relaxation does not occur at this temperature. The maximum stress recovery values at 45°C for 40% and 60% deformations are read 3.28 and 5.63 MPa, respectively. According to Figure 10 (b), with the increase in temperature from 45°C to 65°C, the stress recovery increases for both samples, and the maximum values are reached at 65°C. The amount of stress recovery decreases over time at a constant temperature of 65°C. The maximum stress recovery for 40% and 60% deformations are

measured 5.28 and 8.74 MPa, respectively. In addition, the amount of stress relaxation and the decreasing rate is very small and similar for both samples.

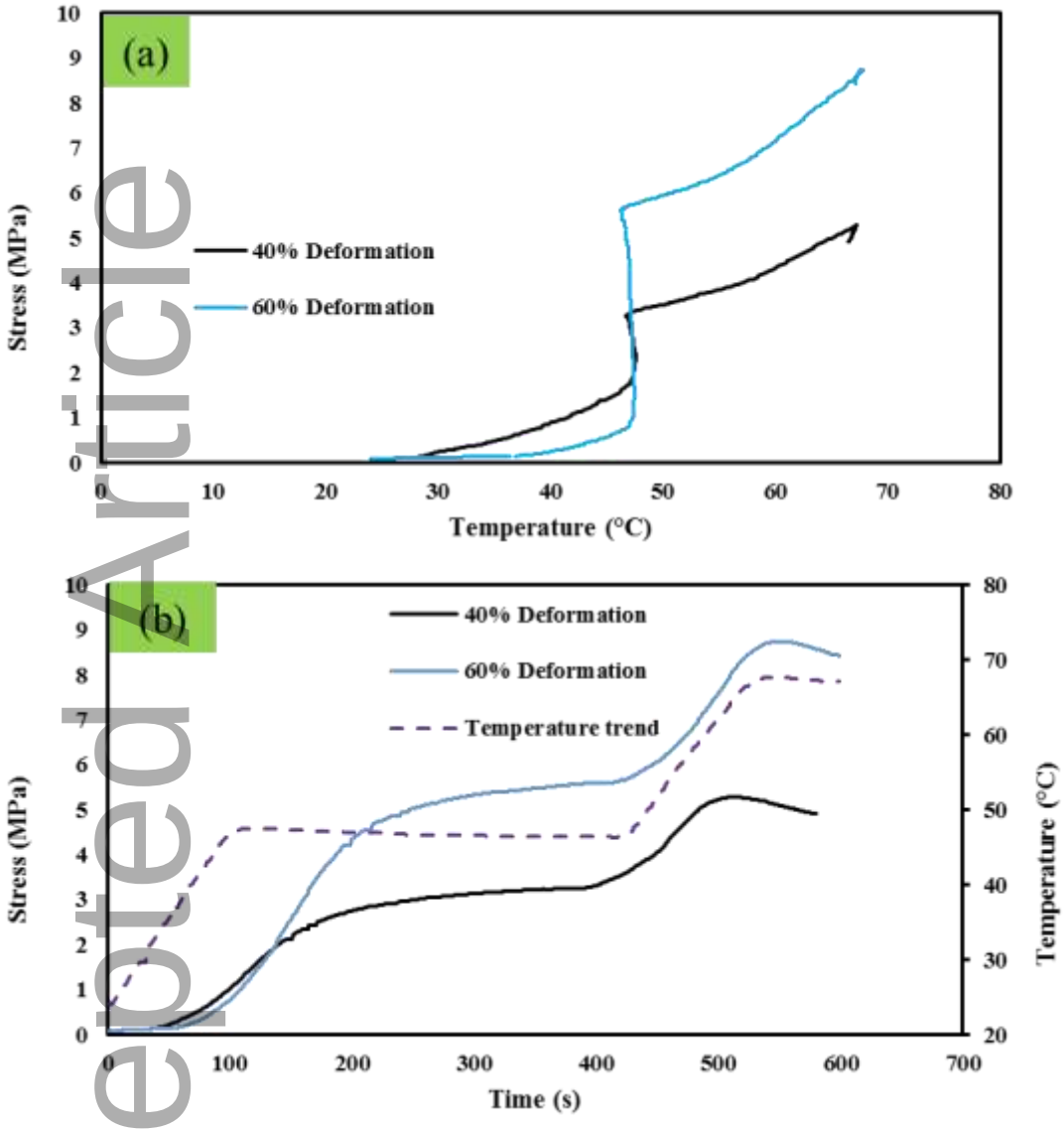


**Figure 10.** Influence of programming deformations on the stress recovery according to (a) temperature and (b) time.

### *3-5-3- Effect of load holding time*

As a result, increasing the load holding time can have a destructive effect on the stress recovery behaviour. According to Table 5, the maximum stress recovery values at two recovery temperatures of 45°C and 65°C for the hot programmed PVC-PCL10 sample are 3.26MPa and 7.72 MPa,

respectively. They are reduced by 42% and 11%, respectively, compared to the hot programmed sample without load holding time. First, a longer load holding time acts like higher programming temperatures and heating and cooling rate, or a lower deformation speed, which are other thermo-temporal conditions. For this purpose, they follow the same concept based on relative molecular mobility and relaxation mechanism and can be implemented interchangeably [37][40][41].

It should be considered that physical crosslinks of molecular entanglements and ordered regions like mesomorphs and crystallites have a finite lifetime that depends on thermo-temporal conditions [37][44]. Higher load holding time leads to more efficient stress relaxation of programmed SMP and more stability in the deformed state, but the dominant relaxation mechanism is different at various temperatures [39][40]. As mentioned, 42% and 11% decrease in the stress recovery at 45°C and 65°C is due to greater stability in the deformed state and the increase in the stress relaxation rate is due to the intensification of relaxation mechanisms with the addition of load holding time [45][46].

### *3-5-4- Recovery temperature*

Figure 11 shows the changes in stress recovery in terms of temperature and time for the PVC-PCL10 hot programmed at two recovery temperatures of 45°C and 65°C. According to Figure 11(a), with the increase in recovery temperature from 45°C to 65°C, the amount of stress recovery increases. The maximum value of stress recovery in these two temperatures is 5.63 and 7.92 MPa respectively. In Figure 11(b), the stress recovery changes in terms of time are presented, based on which the stress recovery slope is higher at 65°C. In fact, with the increase in temperature, in addition to the maximum stress recovery, the stress recovery rate also increases. The changes of the stress recovery upon reaching constant temperatures of 45°C and 65°C have two different trends. At a fixed recovery temperature of 45°C, the amount of stress recovery increases continuously and gradually over time. This stress recovery mechanism is of great interest for medical applications. However, at a constant recovery temperature of 65°C, the stress recovery reaches the maximum value and then decreases at

a low rate, which can be due to the effect of time on the drop in elastic modulus and may also be caused by the activation of relaxation mechanisms (opening of molecular entanglements).

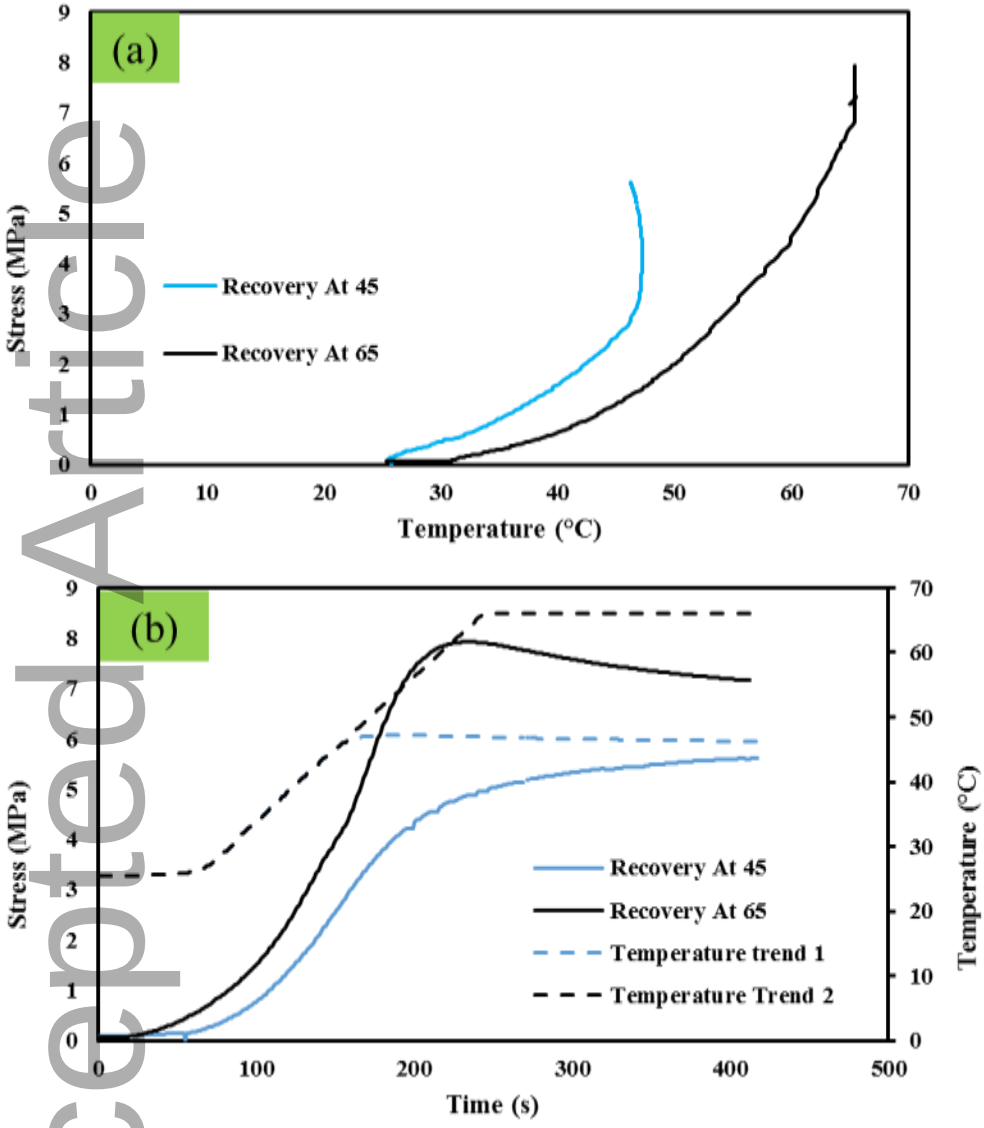


**Figure 11.** Influence of the recovery temperature on the stress recovery according to (a) temperature and (b) time.

### *3.6. SEM*

In Figure 12, SEM images of the macro and microstructure of 3D printed two PVC-PCL compounds are presented to examine the printability, morphology and miscibility of PVC-PCL blends. According to Figure 12(a), the PVC-PCL5 sample has medium printability, and by increasing

the amount of PCL to 10%wt (Figure 12(d)), the adhesion between the raster and layers improves and the density of microholes decreases. Of course, the FFF mechanism (feeding system and fast cooling) has a great contribution to the formation of these microholes [47]–[49]. As can be found, the SEM images confirm the results of the DMTA test and the miscible morphology for both PVC-PCL compounds. Of course, according to Figure 12 (b) and (c), phase separation is observed in some droplets or even regions for the PVC-PCL5. But based on Figure 12 (e) and (f) in the PVC-PCL10, almost a completely single-phase morphology is observed, which indicates the high solubility of PVC and PCL. The high compatibility of the raw materials up to the molecular level and the proximity of the solubility parameters of the two materials are the main reasons for obtaining the miscible morphology. It can cause more favorable printability, mechanical and thermomechanical properties due to the creation of a homogeneous and uniform microstructure.

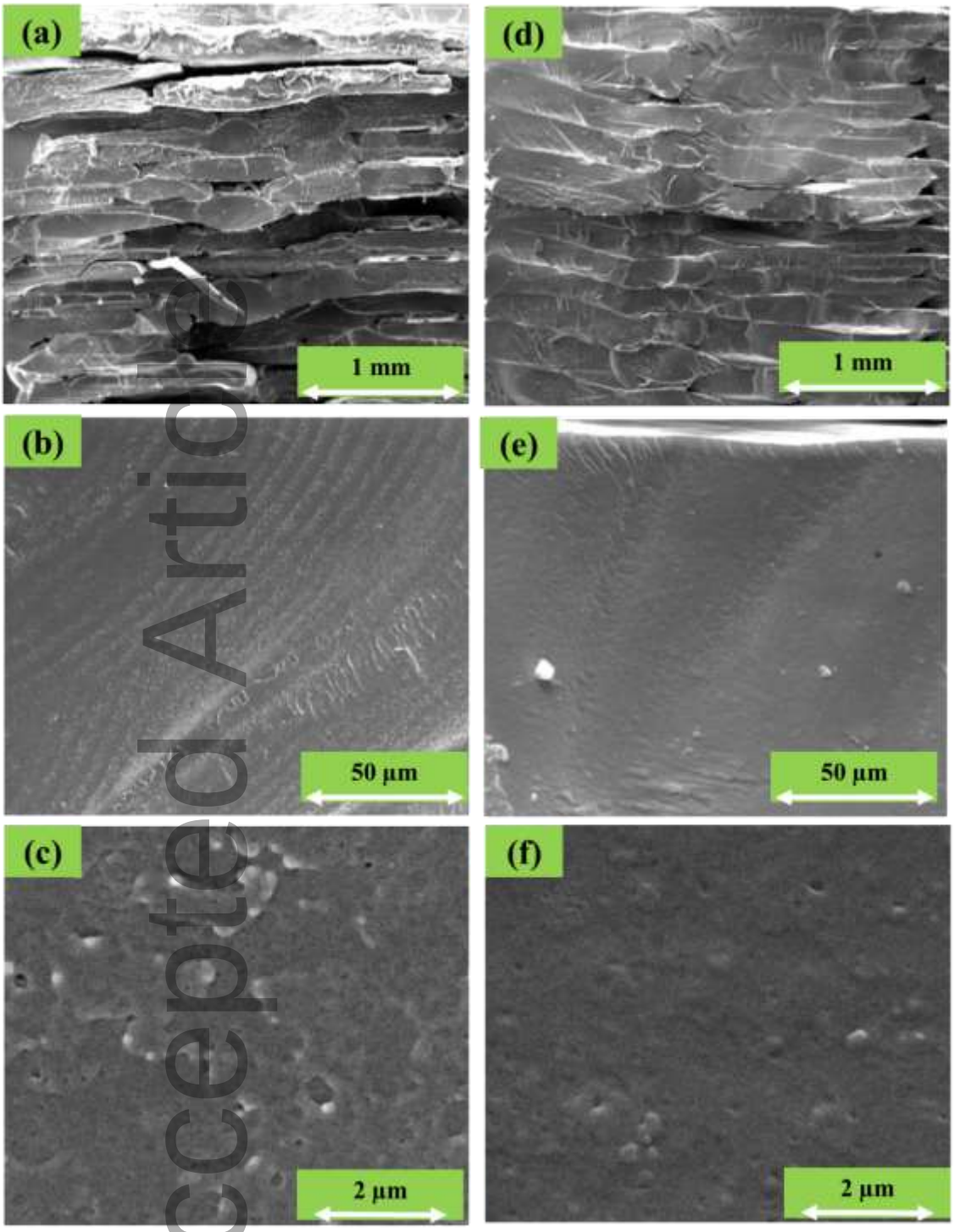


**Figure 12.** SEM images of two PVC-PCL compounds to examine the morphology and miscibility:

## 4- Conclusion

The main aim of this research was to provide an insightful understanding of shape memory behaviors of bio-compatible PVC-PCL blends 4D printed by FFF and programmed under different thermo-mechanical protocols. A detailed analysis of the influence of programming parameters on the shape

memory performance in terms of shape fixity, shape recovery, stress recovery and stress relaxation was carried out.

- DMTA and SEM revealed that the PVC-PCL compounds have an acceptable miscibility, and the miscibility value improves with the increase PCL from 5wt% to 10wt%. Also, with an increase in the amount of PCL, the printability enhances, while the transition temperature decreases. PVC-PCL10 with the glass-to-rubber transition temperature of 37°C and biocompatibility could pave the way for 4D printing of shape adaptive soft devices specially those for biomedical applications and served in the body temperature.
- The 4D printed PVC-PCL SMP demonstrated a high level of shape fixity and shape recovery. In all three thermal regions, the shape fixity values were higher for the PVC-PCL5 compound, and both PVC-PCL compounds have full shape recovery (100%). Also, the effect of programming temperature on shape memory properties was much more visible and tangible than the effect of chemical composition in PVC-PCL blends.
- The shape fixity values for cold, warm, and hot programmed PVC-PCL10 samples were 54.04%, 66.55%, and 88.14%, respectively. Taking into account 10 minutes' load holding time, the amount of shape fixity reached 100%, and on the other hand, the amount of shape recovery decreased. With the increase of deformation from 40% to 60%, the shape fixity decreased from 91.03% to 88.14%. This decreasing trend in shape recovery was also observed in both recovery temperatures.
- Cold programmed PVC-PCL10 samples had the highest stress recovery at 45°C. Considering the recovery temperature of 45°C for PVC-PCL10, which is its glass transition zone, the stress relaxation rate was very low, and it can be the excellent performance for medical applications in the body temperature range.

- Hot programmed samples had the highest stress recovery at 65°C and showed the best stress relaxation performance at both recovery temperatures. With the increase in recovery temperature from 45°C to 65°C, the amount of stress recovery increased. The maximum value of stress recovery in these two temperatures was 5.63 and 7.92 MPa respectively.

- The developed shape memory blend with excellent 4D printability and performance could be instrumental in 4D printing shape adaptive structures like shape-memory intervertebral cages as spinal support devices.



**References**


[1] S. Yang, Y. Zhang, Z. Sha, Z. Huang, H. Wang, F. Wang, J. Li, *ACS Appl. Mater. Interfaces* **2022**.

[2] J. Gan, F. Li, K. Li, E. Li, B. Li, *Compos. Sci. Technol.* **2023**, *234*, 109928.

[3] C. Xiao, K. Zheng, S. Chen, N. Li, X. Shang, F. Wang, J. Liang, S.B. Khan, Y. Shen, B. Lu, H. Ma, Z. Chen, *Addit. Manuf.* **2023**, *71*, 103607.

[4] Z. Li, J. Liang, L. Lu, L. Liu, L. Wang, *Int. J. Biol. Macromol.* **2024**, *266*, 131279.

[5] Y. Xu, F. Zhang, W. Zhai, S. Cheng, J. Li, Y. Wang, *Polym. 2022, Vol. 14, Page 566* **2022**, *14*, 566.

[6] M. Joyce, T. Hodgkinson, M. Lemoine, A. González-Vázquez, D.J. Kelly, F.J. O'Brien, *Eur. Cells Mater.* **2023**, *45*, 158.

[7] S.J. Kim, M.G. Kim, J. Kim, J.S. Jeon, J. Park, H.G. Yi, *Cyborg Bionic Syst.* **2023**, *4*.

[8] M.A. Kouka, F. Abbassi, M. Habibi, F. Chabert, A. Zghal, C. Garnier, *Adv. Eng. Mater.* **2023**, *25*, 2200650.

[9] M. Aberoumand, D. Rahmatabadi, K. Soltanmohammadi, E. Soleyman, I. Ghasemi, M. Baniassadi, K. Abrinia, M. Bodaghi, M. Baghani, *Sensors Actuators A Phys.* **2023**, *361*, 114572.

[10] D. Rahmatabadi, K. Soltanmohammadi, M. Aberoumand, E. Soleyman, I. Ghasemi, M. Baniassadi, K. Abrinia, M. Bodaghi, M. Baghani, *Phys. Scr.* **2024**, *99*, 025013.

[11] D. Rahmatabadi, M. Aberoumand, K. Soltanmohammadi, E. Soleyman, I. Ghasemi, M. Baniassadi, K. Abrinia, M. Bodaghi, M. Baghani, *Adv. Eng. Mater.* **2023**, *25*, 2201309.

[12] A. Tariq, Z.U. Arif, M.Y. Khalid, M. Hossain, P.I. Rasool, R. Umer, S. Ramakrishna, *Adv. Eng. Mater.* **2023**, *25*, 2301074.

[13] W. Zhao, J. Zhu, L. Liu, J. Leng, Y. Liu, *Int. J. Smart Nano Mater.* **2023**, *14*, 1.

[14] M. Song, X. Liu, H. Yue, S. Li, J. Guo, *Polymer (Guildf).* **2022**, *256*, 125190.

[15] G. Li, A. Wang, *J. Polym. Sci. Part B Polym. Phys.* **2016**, *54*, 1319.

[16] E. Soleyman, D. Rahmatabadi, K. Soltanmohammadi, M. Aberoumand, I. Ghasemi, K. Abrinia, M. Baniassadi, K. Wang, M. Baghani, *Smart Mater. Struct.* **2022**, *31*, 085002.

[17] P. Wu, T. Yu, M. Chen, D. Hui, *J. Manuf. Process.* **2022**, *84*, 1507.

[18] L. Huang, R. Jiang, J. Wu, J. Song, H. Bai, B. Li, Q. Zhao, T. Xie, L.M. Huang, J.J. Wu, H. Bai, B.G. Li, Q. Zhao, T. Xie, R.Q. Jiang, Z. Song, *Adv. Mater.* **2017**, *29*, 1605390.

[19] F. Yang, S. Zhang, J.C.M. Li, *J. Electron. Mater. 1997 267* **1997**, *26*, 859.

[20] F. Yang, J.C.M. Li, *J. Mater. Res. 1997 1210* **2011**, *12*, 2809.

[21] X.L. Wu, T.X. Wang, W.M. Huang, Y. Zhao, *Appl. Sci. 2017, Vol. 7, Page 848* **2017**, *7*, 848.

[22] W. Liu, R. Zhang, M. Huang, X. Dong, W. Xu, N. Ray, J. Zhu, *Polymer (Guildf).* **2016**, *104*, 115.

[23] M.E. Pekdemir, E. Öner, M. Kök, I.N. Qader, *Iran. Polym. J. 2021 306* **2021**, *30*, 633.

[24] M. Ehteramian, I. Ghasemi, H. Azizi, M. Karrabi, *Iran. Polym. J. 2021 304* **2021**, *30*, 411.

[25] H. Mo Jeong, J.H. Song, Y. Sang, B. Lee, K. Kyu, **n.d.**

[26] T.X. Wang, L.L. Chang, Y.H. Geng, X. Shen, *Polym. 2020, Vol. 12, Page 2025* **2020**, *12*, 2025.

[27] V. Skákalová, V. Lukeš, M. Breza, *Macromol. Chem. Phys.* **1997**, *198*, 3161.

[28] N. Alikarami, M. Abrisham, X. Huang, M. Panahi-Sarmad, K. Zhang, K. Dong, X. Xiao, *Int. J. Smart Nano Mater.* **2022**, *13*, 130.

[29] K. Mirasadi, D. Rahmatabadi, I. Ghasemi, M. Khodaei, M. Baniassadi, M. Baghani, *Macromol. Mater. Eng.* **2024**, 2400038.

[30] F. Chiellini, M. Ferri, A. Morelli, L. Dipaola, G. Latini, *Prog. Polym. Sci.* **2013**, *38*.

[31] D.E. Skillicorn, G.G.A. Perkins, A. Slark, J. V. Dawkins, *J. Vinyl Technol.* **1993**, *15*, 105.

[32] R.E. Prud'homme, *Polym. Eng. Sci.* **1982**, *22*.

[33] L.M. Robeson, *J. Vinyl Technol.* **1990**, *12*, 89.

[34] M. Aberoumand, K. Soltanmohammadi, D. Rahmatabadi, E. Soleyman, I. Ghasemi, M. Baniassadi, K. Abrinia, M. Bodaghi, M. Baghani, *Macromol. Mater. Eng.* **2023**, *308*, 2200677.

[35] J.D. Ferry, *Wiley, New York* **1980**, 672.

[36] D. Gutierrez-Lemini, *Eng. Viscoelasticity* **2014**, 1.

[37] T.D. Nguyen, H. Jerry Qi, F. Castro, K.N. Long, *J. Mech. Phys. Solids* **2008**, *56*, 2792.

[38] M. Aberoumand, K. Soltanmohammadi, E. Soleyman, D. Rahmatabadi, I. Ghasemi, M. Baniassadi, K. Abrinia, M. Baghani, *J. Mater. Res. Technol.* **2022**, *18*, 2552.

[39] H. Tobushi, R. Matsui, S. Hayashi, D. Shimada, *Smart Mater. Struct.* **2004**, *13*, 881.

[40] H. Tobushi, S. Hayashi, K. Hoshio, N. Miwa, *Smart Mater. Struct.* **2006**, *15*, 1033.

[41] K. Yu, H.J. Qi, *Soft Matter* **2014**, *10*, 9423.

[42] Jatin, V. Sudarkodi, S. Basu, *Int. J. Plast.* **2014**, *56*, 139.

[43] J. Zhang, X. Zhang, Z. zhang Wang, H. yu Li, *Mech. Time-Dependent Mater.* **2022**.

[44] V.G. Rostiashvili, T.A. Vilgis, *Encycl. Polym. Nanomater.* **2020**, 1.

[45] K. Yu, Q. Ge, H.J. Qi, *Nat. Commun.* **2014**, *5*, 1.

[46] X. Zhang, Z. Tang, B. Guo, *J. Polym. Sci. Part B Polym. Phys.* **2016**, *54*, 1295.

[47] J. Ghorbani, P. Koirala, Y.-L. Shen, M. Tehrani, *J. Manuf. Process.* **2022**, *80*, 651.

[48] D. Rahmatabadi, I. Ghasemi, M. Baniassadi, K. Abrinia, M. Baghani, *J. Mater. Res. Technol.* **2022**, *21*, 3970.

[49] D. Rahmatabadi, K. Soltanmohammadi, M. Aberoumand, E. Soleyman, I. Ghasemi, M. Baniassadi, K. Abrinia, M. Bodaghi, M. Baghani, *Macromol. Mater. Eng.* **2023**, *308*, 2200568.

This work introduces a new class of bio-compatible shape memory polymers by blending PVC and PCL. Thermo-mechanical and morphological analyses reveal their excellent 4D printability and performance in terms of programmability, compressive shape recovery, shape fixity, working temperature, and stress relaxation. This 4D printing would be instrumental for many applications like fabricating customized shape-memory intervertebral cages as spinal support devices.